gle-ion mechanism the relevant point group is that at the Mn center, namely, C_2. A quick inspection shows that for pair transitions this leads to the same orbital selection rules as the exchange mechanism. These rules are collected in Table I.

Beside these purely qualitative arguments, we get some quantitative ideas about relative intensities by considering their physical origins. The main source of intensity for the single-ion mechanism is the parity-allowed transitions in the UV region, namely, ligand-to-metal charge-transfer transitions and metal-centered d-p transitions. Both of these sources are expected to lead to a fairly isotropic intensity distribution, because the centers are very close to octahedral. In the Tanabe mechanism ligand-to-metal as well as high-lying metal-to-metal transitions can contribute to the intensity of pair transitions. Whereas the former should lead to a more or less isotropic transition moment, the latter are restricted to the hexagonal plane and should contribute only to the σ intensity.

The overall spectra in Figures 1 and 2 show a predominance of σ intensity in the whole spectral range. $^4T_1(G)$ in the chloride host is the only band with comparable intensity in σ and π. This dominance in σ, together with the absolute intensity of the bands (approximately 1 order of magnitude more intense than in mononuclear Mn(II) complexes), is a clear indication of a dominant exchange mechanism.

Further support for this comes from the observed drastic intensity decrease of *all the band systems* when the crystals are cooled below 4 K. The relative populations of the singlet and triplet dimer levels show the largest variations in this temperature range. In the $^4A_1{}^4E$ region, a satisfactory analysis of the data is possible by assuming that there is no singlet intensity. The behaviors in the $^4T_2(D)$ and $^4E(D)$ regions are similar. We conclude therefore that the exchange mechanism dominates the spectrum.

Acknowledgment. We thank Naomi Furer for preparing the crystals used in this study. P.J.M. is also grateful for support from a Canisius College Summer Faculty Fellowship. Financial support by the Swiss National Science Foundation is acknowledged.

Contribution from The Institute for Cancer Research, Philadelphia, Pennsylvania 19111, and Department of Chemistry, Columbia University, New York, New York 10027

Crystal and Molecular Structure of a Chiral-Specific DNA-Binding Agent: Tris(4,7-diphenyl-1,10-phenanthroline)ruthenium(II)

Barry M. Goldstein,† Jacqueline K. Barton,‡ and Helen M. Berman*

Received July 23, 1985

The crystal and molecular structure of the cationic coordination complex tris(4,7-diphenyl-1,10-phenanthroline)ruthenium(II), $Ru(DIP)_3^{2+}$, has been determined. The complex crystallizes in the monoclinic space group $P2_1/c$ with cell dimensions a = 13.085 (2) Å, b = 24.173 (1) Å, c = 22.773 (4) Å, β = 110.91 (1)°, and Z = 4. The final R value is 0.082. All the phenyl groups are skew to the phenanthroline ligands. There are no stacking interactions in the crystal. A plausible model for the Δ enantiomer binding to right-handed DNA is proposed.

Introduction

The cationic coordination complex tris(4,7-diphenyl-1,10-phenanthroline)ruthenium(II), $Ru(DIP)_3^{2+}$, shows chiral discrimination in binding to different forms of DNA.[1] The Ru-

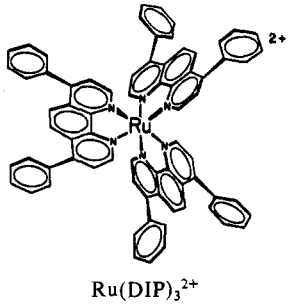

$Ru(DIP)_3^{2+}$

$(DIP)_3^{2+}$ complex possesses both Δ and λ enantiomers due to the asymmetric center at the six-coordinate ruthenium atom. Spectrophotometric studies have shown that both the Δ and λ isomers bind to left-handed Z-DNA.[1a] However, only the Δ enantiomer binds to right-handed B-DNA.[1b] Hence, the stereospecific preferential binding of the λ isomer to Z-DNA provides a molecular probe to distinguish between left- and right-handed DNA helices.[1c]

The development of new chiral probes for DNA that are conformation- and site-specific requires detailed structural information about the metal complexes. As part of an effort to model the binding of $Ru(DIP)_3^{2+}$ to DNA, the structure of the $Ru(DIP)_3^{2+}$ complex has been determined with use of single-crystal X-ray diffraction techniques. On the basis of the structure described here, a more chemically sound model for the binding of $Ru(DIP)_3^{2+}$ to the DNA helix may be considered.

Experimental Section

X-ray Data Collection. Racemic $Ru(DIP)_3^{2+}$ dichloride, $Ru[(C_{12}N_2H_6)(C_6H_5)_2]_3Cl_2$ was obtained as described by Lin et al.[2] A single large red plate (0.5 mm × 0.35 mm × 0.10 mm) was grown by very slow evaporation of a 10 mM solution of the racemic complex in a 24% water/76% methanol (v/v) mixture at 4 °C. The crystal was mounted in a 0.7-mm glass capillary tube containing a strip of filter paper saturated with mother liquor. A preliminary rapid data scan by diffractometer revealed a monoclinic crystal system. The only observed systematic absences were $0k0$ for $k = 2n + 1$ and $h0l$ for $l = 2n + 1$, indicating unambiguously space group $P2_1/c$. Cell dimension and intensity data were collected at 4 °C with use of an Enraf-Nonius CAD-4 diffractometer equipped with a locally designed cooling device[3] and graphite-monochromatized Cu Kα radiation. Lattice constants were obtained by least-squares refinement of the angular settings of 25 reflections in the range θ = 25-30°. The resulting values are a = 13.085 (2) Å, b = 24.173 (1) Å, c = 22.773 (4) Å, β = 110.91 (1)°, and Z = 4. Reflections were measured in the quadrant $(\pm h,-k,l)$ with use of the ω-2θ scan method with a variable scan width $\Delta\omega = (1.75 + 0.15 \tan\theta)°$, this angle being extended 25% on each side for background measurements. The scan rate varied between 1.0 and 4.0° min^{-1} depending upon the value of $\sigma(I)/I$ for each reflection. Data were collected in incremental shells in the range

* To whom correspondence should be addressed at The Institute for Cancer Research.

† Present address: Department of Pharmacology, School of Medicine and Dentistry, University of Rochester, Rochester, NY 14642.

‡ Columbia University.

(1) (a) Barton, J. K.; Basile, L. A.; Danishefsky, A.; Alexandrescu, A. *Proc. Natl. Acad. Sci. U.S.A.* **1984**, *81*, 1961-1965. (b) Kumar, C.; Barton, J. K.; Turro, N. J. *J. Am. Chem. Soc.* **1985**, *107*, 5518-5523. (c) Barton, J. K.; Raphael, A. *J. Am. Chem. Soc.* **1984**, *106*, 2466-2468.

(2) Lin, C. T.; Bottcher, W.; Chou, M.; Creutz, C.; Sutin, N. *J. Am. Chem. Soc.* **1976**, *98*, 6536-6544.

(3) Takusagawa, F. Technical Report ICR-1982-0001-0001-01; The Institute for Cancer Research: Fox Chase, PA, 1982.

0020-1669/86/1325-0842$01.50/0

Table I. Atomic Coordinates for $Ru(DIP)_3^{2+}$

atom	x/a	y/b	z/c	atom	x/a	y/b	z/c
Ru	0.0435 (1)	0.2521 (1)	0.1326 (1)	Cp(9)	−0.524 (1)	0.4151 (7)	0.1561 (8)
N(1)	0.108 (1)	0.2968 (6)	0.2148 (6)	Cp(10)	−0.560 (1)	0.3854 (7)	0.1978 (8)
C(2)	0.213 (1)	0.3019 (7)	0.2502 (9)	Cp(11)	−0.502 (1)	0.3392 (7)	0.2287 (8)
C(3)	0.244 (2)	0.3307 (8)	0.3082 (10)	Cp(12)	−0.408 (1)	0.3226 (7)	0.2180 (8)
C(4)	0.170 (1)	0.3551 (7)	0.3300 (8)	Cp(1)	0.203 (2)	0.3824 (8)	0.3916 (9)
C(4a)	0.055 (1)	0.3517 (7)	0.2879 (9)	Cp(2)	0.294 (2)	0.4213 (9)	0.4087 (10)
C(5)	−0.030 (2)	0.3769 (9)	0.3033 (10)	Cp(3)	0.326 (2)	0.4455 (10)	0.4684 (12)
C(6)	−0.131 (2)	0.3722 (8)	0.2664 (9)	Cp(4)	0.279 (2)	0.4306 (10)	0.5108 (12)
C(6a)	−0.165 (1)	0.3399 (7)	0.2092 (9)	Cp(5)	0.195 (2)	0.3944 (11)	0.4964 (13)
C(7)	−0.276 (2)	0.3327 (7)	0.1640 (9)	Cp(6)	0.155 (2)	0.3663 (10)	0.4363 (11)
C(8)	−0.291 (2)	0.3019 (8)	0.1103 (9)	Cp(7″)	−0.178 (1)	0.0771 (7)	−0.0848 (8)
C(9)	−0.200 (1)	0.2786 (8)	0.0971 (8)	Cp(8″)	−0.283 (2)	0.0855 (9)	−0.1250 (11)
N(10)	−0.098 (1)	0.2859 (5)	0.1388 (6)	Cp(9″)	−0.330 (2)	0.0433 (11)	−0.1720 (13)
C(10a)	−0.082 (1)	0.3177 (7)	0.1946 (8)	Cp(10″)	−0.272 (2)	−0.0028 (10)	−0.1756 (12)
C(1a)	0.026 (1)	0.3210 (7)	0.2308 (8)	Cp(11″)	−0.171 (2)	−0.0114 (9)	−0.1359 (11)
N(1′)	0.190 (1)	0.2278 (5)	0.1296 (7)	Cp(12″)	−0.119 (2)	0.0301 (8)	−0.0905 (9)
C(2′)	0.248 (1)	0.1816 (7)	0.1552 (9)	Cp(1″)	−0.083 (1)	0.0359 (5)	0.2486 (7)
C(3′)	0.347 (1)	0.1681 (8)	0.1439 (10)	Cp(2″)	−0.195 (1)	0.0267 (5)	0.2347 (7)
C(4′)	0.385 (1)	0.2012 (8)	0.1060 (11)	Cp(3″)	−0.229 (1)	−0.0170 (5)	0.2632 (7)
C(4a′)	0.329 (1)	0.2501 (11)	0.0829 (7)	Cp(4″)	−0.152 (1)	−0.0514 (5)	0.3056 (7)
C(5′)	0.365 (2)	0.2932 (9)	0.0514 (10)	Cp(5″)	−0.041 (1)	−0.0422 (5)	0.3195 (7)
C(6′)	0.311 (1)	0.3431 (7)	0.0298 (10)	Cp(6″)	−0.006 (1)	0.0014 (5)	0.2911 (7)
C(6a′)	0.208 (1)	0.3513 (7)	0.0409 (9)	Cp(1′)	0.480 (1)	0.1849 (7)	0.0915 (8)
C(7′)	0.144 (1)	0.3998 (8)	0.0218 (9)	Cp(2′)	0.578 (1)	0.1699 (7)	0.1391 (8)
C(8′)	0.047 (2)	0.404 (8)	0.029 (1)	Cp(3′)	0.667 (1)	0.1524 (7)	0.1239 (8)
C(9′)	0.012 (2)	0.3615 (7)	0.0599 (9)	Cp(4′)	0.658 (1)	0.1498 (7)	0.0612 (8)
N(10′)	0.072 (1)	0.3164 (5)	0.0812 (7)	Cp(5′)	0.561 (1)	0.1648 (7)	0.0136 (8)
C(10a′)	0.170 (1)	0.3106 (7)	0.0719 (8)	Cp(6′)	0.472 (1)	0.1823 (7)	0.0288 (8)
C(1a′)	0.230 (1)	0.2629 (5)	0.0939 (7)	Cp(7′)	0.180 (1)	0.4457 (6)	−0.0108 (8)
N(1″)	0.016 (1)	0.1823 (6)	0.1772 (7)	Cp(8′)	0.190 (1)	0.4968 (6)	0.0191 (8)
C(2″)	0.040 (2)	0.1779 (8)	0.2420 (8)	Cp(9′)	0.223 (1)	0.5432 (6)	−0.0058 (8)
C(3″)	0.002 (2)	0.1270 (10)	0.2641 (12)	Cp(10′)	0.247 (1)	0.5384 (6)	−0.0606 (8)
C(4″)	−0.048 (2)	0.0846 (8)	0.2222 (10)	Cp(11′)	0.237 (1)	0.4873 (6)	−0.0906 (8)
C(4a″)	−0.064 (2)	0.0905 (7)	0.1597 (8)	Cp(12′)	0.203 (1)	0.4410 (6)	−0.0657 (8)
C(5″)	−0.113 (2)	0.0487 (7)	0.1126 (10)	Cl	0.054 (1)	0.2215 (6)	0.3929 (6)
C(6″)	−0.131 (2)	0.0555 (7)	0.0504 (10)	Solv(1)	0.278 (2)	0.1971 (10)	0.3755 (11)
C(6a″)	−0.100 (1)	0.1080 (7)	0.0295 (8)	Solv(2)	0.296 (2)	0.1060 (11)	0.2936 (13)
C(7″)	−0.125 (2)	0.1192 (7)	−0.0362 (8)	Solv(3)	0.482 (2)	0.6553 (11)	0.0378 (13)
C(8″)	−0.104 (2)	0.1713 (7)	−0.0526 (10)	Solv(4)	0.553 (3)	0.7761 (15)	0.6963 (16)
C(9″)	−0.054 (1)	0.2108 (7)	−0.0038 (8)	Solv(5)[a]	0.500 (6)	0.5626 (28)	0.0767 (32)
N(10″)	−0.030 (1)	0.2008 (5)	0.0568 (6)	Solv(6)[a]	0.485 (6)	0.5903 (31)	0.2142 (33)
C(10a″)	−0.055 (1)	0.1488 (6)	0.0722 (7)	Solv(7)	0.274 (3)	0.8026 (15)	0.5542 (17)
C(1a″)	−0.033 (1)	0.1410 (7)	0.1373 (7)	Solv(8)[a]	0.339 (6)	0.7390 (25)	0.5948 (29)
Cp(7)	−0.372 (1)	0.3523 (7)	0.1763 (8)	Solv(9)[a]	0.125 (6)	0.6265 (27)	0.1103 (31)
Cp(8)	−0.430 (1)	0.3985 (7)	0.1454 (8)	Solv(10)	0.185 (3)	0.7669 (16)	0.6949 (18)

[a] Set at $^1/_2$ occupancy.

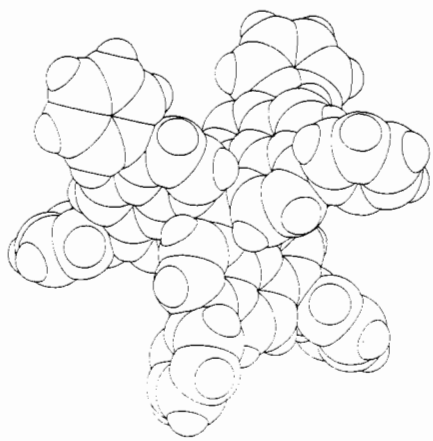

Figure 1. Space-filling diagram of $Ru(DIP)_3^{2+}$. Hydrogen atoms are included.

$2° < \theta < 55°$, yielding a total of 8430 unique reflections. Of these, 3031 had values of $|F_o|^2 > 3\sigma(F_o^2)$, where $\sigma(F_o^2) = [\sigma^2(I) + (0.02|F_o|^2)^2]^{1/2}$, and were used in the subsequent refinement.

Three standard reflections measured every 3 h of X-ray exposure time showed an average 14% decline in intensity over the course of the data collection. A separate linear decay correction was applied to the set of reflections collected within each 2-h time period. Corrections for Lorentz and polarization factors were applied, and in addition, data were corrected for absorption with use of the semiempirical ψ-scan technique.[4] A single ψ scan was employed, consisting of 36 measurements of a standard reflection in 10° steps of ϕ with the crystal in an approximate equiinclination setting.

Structure Solution and Refinement. The structure was solved by Patterson and Fourier techniques. The position of the ruthenium atom was determined from the three-dimensional Patterson map. Subsequent Fourier maps yielded the remainder of the complex.

The structure was refined with use of blocked-full-matrix least-squares techniques. The function minimized was $\sum w(\Delta F^2)$, where $\Delta F = |F_o| - |F_c|$ with weights $w = k/\sigma^2$. The value of k was obtained by minimization of the function $|\Delta F|^2 - \sigma^2/k$, where $\sigma = \sigma(F_o^2)/2|F_o|$ and $\sigma(F_o^2)$ is defined as above. The ruthenium atom and all atoms in the three phenanthroline groups were refined anisotropically. Because of relatively large thermal motion, four of the six phenyl groups were refined as rigid bodies, with only a torsion rotation allowed about the bond between the phenyl group and the phenanthroline moiety. Atoms in the phenyl groups, including those in the four constrained moieties, were refined with isotropic temperature factors.

Difference and Fourier maps computed throughout the refinement consistently indicated a disordered solvent network. Only one of the two chloride ions was clearly discernible. A number of models were tested in which water molecules and the missing chloride ion were distributed with partial occupancies over multiple sites. However, it was not possible to distinguish between these models by either stereochemical criteria or refinement results. Thus, all potential solvent sites from the difference map were occupied with oxygen atoms, initially at full occupancy. The positional parameters of these atoms were then allowed to refine with

(4) North, A.; Phillips, D.; Mathews, F. *Acta Crystallogr., Sect. A.: Cryst. Phys., Diffr., Theor. Gen. Crystallogr.* **1968**, *A24*, 351–359.

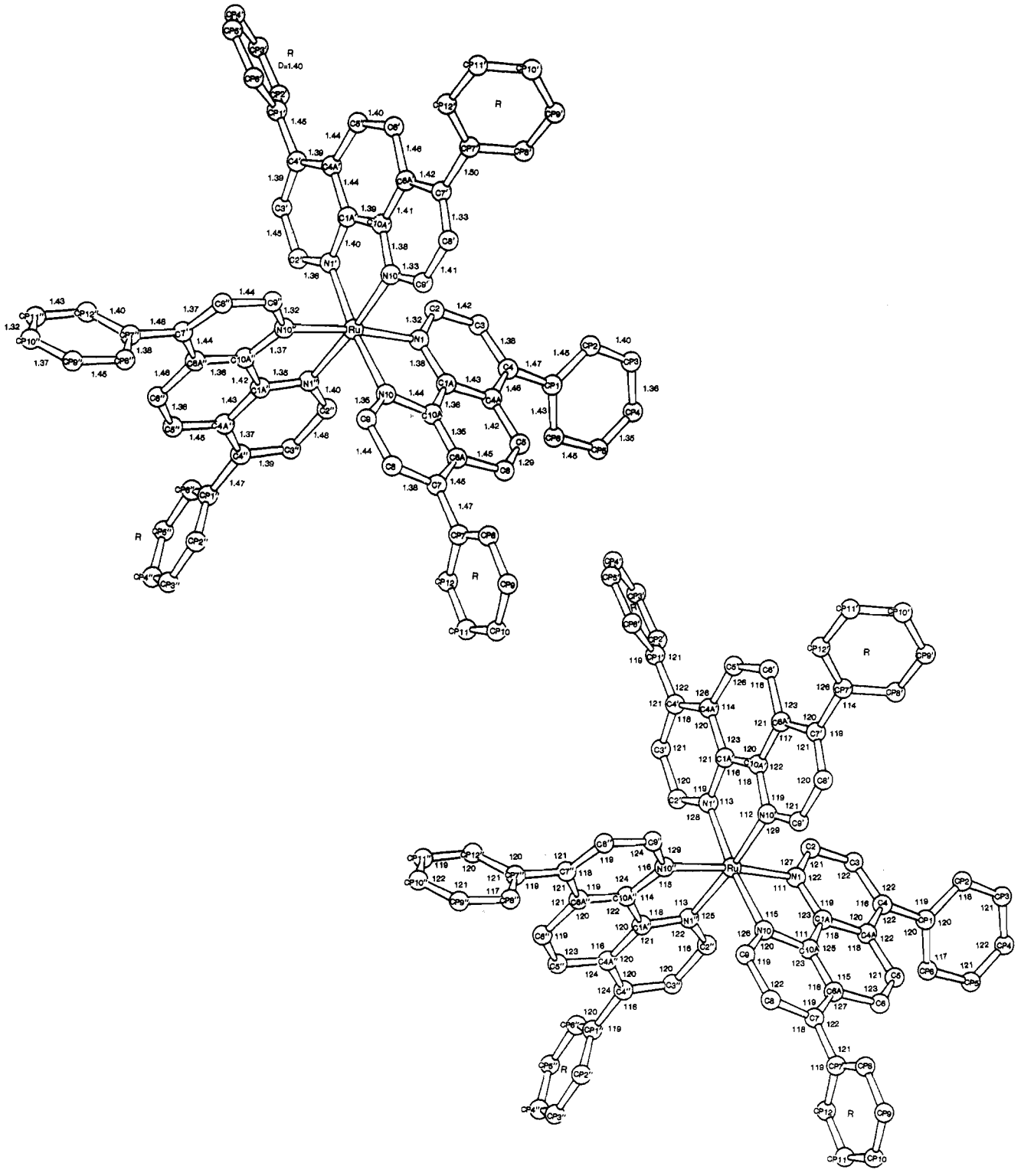

Figure 2. Bond distances (top) (average esd's 0.025 Å) and bond angles (bottom) (average esd's 1.5°) in $Ru(DIP)_3^{2+}$. R indicates that the phenyl group was refined as a rigid body with bond distances of 1.395 Å and angles of 120°. The λ isomer is shown.

unconstrained isotropic temperature factors. The temperature factors of four of these solvent atoms converged to larger values than the others, and the geometry suggested that these were positionally disordered. When the occupancies of these were fixed to 0.5, the temperature factors were refined to values consistent with the rest of the solvent molecules. All solvent sites are labeled Solv in the coordinate list to indicate that they may be partially occupied by disordered water molecules and/or chloride ions.

Final refinements converged to values of $R = 8.2\%$ and $R_w = 7.9\%$, where $R = \sum|\Delta F|/\sum|F_o|$ and $R_w = \sum w^{1/2}|\Delta F|/\sum w^{1/2}|F_o|$. Shifts for most parameters, including those of the disordered solvent, were less than 0.7σ. Atomic scattering factors for all atoms and anomalous dispersion corrections for the ruthenium atom were from ref 5. Following the last cycle of refinement, hydrogen atoms were added to the structure in idealized positions. This was done for graphics and modeling purposes, and no further structure factor or refinement calculations were attempted. Programs used were from the DNA system[6] and SHELX.[7] The final atomic coordinates are given in Table I. The structure factors are deposited as supplementary material.

(5) "International Tables for X-ray Crystallography", 3rd Ed.; Kynoch Press: Birmingham, England, 1974; Vol. IV, pp 99, 149.
(6) Takusagawa, F. "Crystallographic Computing System: DNA"; The Institute for Cancer Research: Fox Chase, PA, 1981.
(7) Sheldrick, G. M. "SHELX76: Program for Crystal Structure Determination"; Cambridge University: Cambridge, England, 1976.

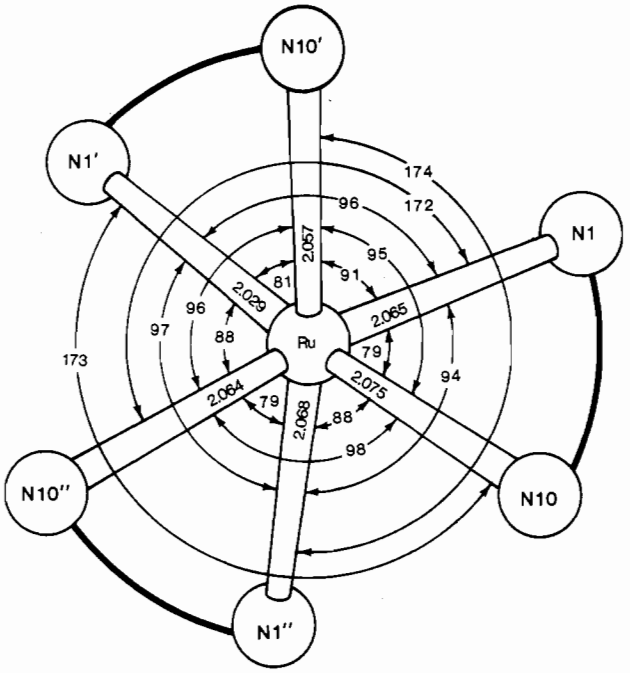

Figure 3. Distances (Å) and angles (deg) involving the ruthenium ion in $Ru(DIP)_3^{2+}$. Average esd's are 0.002 Å and 0.2°, respectively.

Table II. Torsion Angles of Phenyl Groups in $Ru(DIP)_3^{2+}$

atoms	angle, deg
Cp(6)Cp(1)C(4)C(3)	−125
Cp(6′)Cp(1′)C(4′)C(3′)	+127
Cp(6″)Cp(1″)C(4″)C(3″)	−67
Cp(2)Cp(1)C(4)C(3)	+48
Cp(2′)Cp(1′)C(4′)C(3′)	−51
Cp(2″)Cp(1″)C(4″)C(3″)	+108
Cp(8)Cp(7)C(7)C(8)	−79
Cp(8′)Cp(7′)C(7′)C(8′)	+61
Cp(8″)Cp(7″)C(7″)C(8″)	−65
Cp(12)Cp(7)C(7)C(8)	+99
Cp(12′)Cp(7′)C(7′)C(8′)	−120
Cp(12″)Cp(7″)C(7″)C(8″)	+113

Results and Discussion

The $Ru(DIP)_3^{2+}$ molecule consists of three planar phenanthroline groups octahedrally coordinated to the ruthenium atom via their nitrogens. Each phenyl group is skew to the phenanthroline moieties, leading to the appearance of a propeller-like molecule, shown in Figure 1. With few exceptions, all bond lengths and angles related by the approximate mirror symmetry of each phenanthroline group and the approximate threefold rotation axis through the ruthenium atom agree within 3σ (Figure 2). These values are similar to those seen in other metal-coordinated phenanthroline groups.[8-11] As shown in Figure 3, the coordination geometry about the ruthenium atom is that of a distorted octahedron. This is due to the narrow bite of each 1,10-phenanthroline ligand (dark lines), as seen in other ruthenium–phenanthroline complexes.[10,11] The average length of the Ru–N bonds is 2.06 (1) Å. This is between 0.03 and 0.05 Å shorter than that observed when ruthenium is complexed with only one[11] or two[10] phenanthroline moieties. The torsion angles for the phenyl groups show a wide range of values, none of which are close to a 0 or 180° value indicative of a planar conformation (Table II). The crystal itself consists of Δ and Λ molecules arranged such that the hydrophobic aromatic groups are clustered together; none of the phenyl groups are stacked (Figure 4).

Table III. Solvent Contacts Less Than 3.3 Å in the $Ru(DIP)_3^{2+}$ Crystal

atom	atom	dist, Å	symmetry
Cl	Solv(1)	3.14	x, y, z
Cl	Solv(10)	3.07	$-x, 1-y, 1-z$
Cl	Solv(9)	3.26	$-x, -^1/_2+y, ^1/_2-z$
Solv(1)	Solv(3)	3.22	$1-x, -^1/_2+y, ^1/_2-z$
Solv(1)	Solv(4)	3.26	$1-x, 1-y, 1-z$
Solv(2)	Solv(1)	2.95	x, y, z
Solv(2)	Solv(6)	2.95	$1-x, -^1/_2+y, ^1/_2-z$
Solv(3)	Solv(7)	3.06	$x, ^3/_2-y, -^1/_2+z$
Solv(3)	Solv(5)	2.39	x, y, z
Solv(5)	Solv(6)	3.28	x, y, z
Solv(7)	Solv(8)	1.84	x, y, z
Solv(7)	C9	3.28	$-x, ^1/_2+y, ^1/_2-z$
Solv(7)	Solv(9)	3.18	$x, ^3/_2-y, ^1/_2+z$
Solv(8)	Solv(4)	3.06	x, y, z
Solv(9)	C8′	3.25	$-x, 1-y, -z$
Solv(10)	Solv(9)	3.14	$x, ^3/_2-y, ^1/_2+z$

A solvent channel is parallel to the *a* axis and consists of waters of hydration, chloride ions, and possibly methanol molecules.[12] These solvent molecules are connected via intersolvent hydrogen bonds to form a continuous network (Table III, Figure 5). One (of potentially two) chloride ions is clearly identifiable. This forms close contacts (3.07–3.26 Å) with solvent peaks 1, 9, and 10, consistent with chloride–water hydrogen bonds.[13,14] In addition, this ion forms three close contacts (~3.5 Å) with neighboring phenanthroline carbons. The remaining chloride ion is possibly disordered over multiple sites, the most likely being Solv(4), Solv(3), and Solv(2). Each of these sites offers a potential chloride–water hydrogen bond with Solv(1) as well as at least two additional close contacts with neighboring carbons. Solv(7), with its close contact with Solv(8), is also a possible partial-occupancy Cl^- ion. Nevertheless, there are alternative distributions of this ion among the remaining solvent sites. Further, substitutional disorder between chloride ions and water molecules has been observed.[14] Refinement results could not distinguish between these alternatives; hence, no attempt has been made to present a specific disorder model.

The features seen in this crystal and molecular structure can be used to construct models for the binding of $Ru(DIP)_3^{2+}$ with DNA that are consistent with chemical and spectroscopic observations. In one such plausible model (Figure 6) Δ-$Ru(DIP)_3^{2+}$ is bound to a right-handed DNA helix such that a phenanthroline ligand is partially intercalated between the base pairs with one phenyl group in the minor groove (Figure 6a). The other phenyl group and nonintercalating diphenylphenanthroline groups are

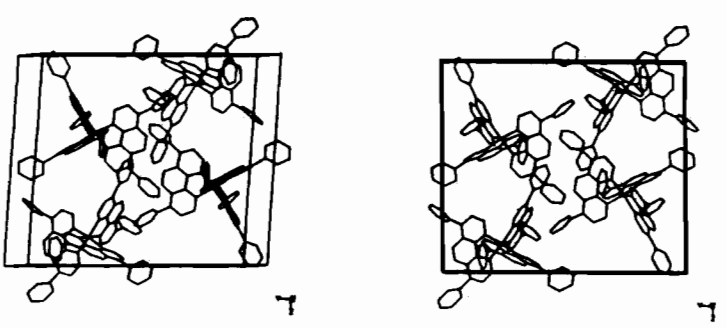

Figure 4. Packing of $Ru(DIP)_3^{2+}$ molecules in the crystal viewed approximately down the *a* axis. Dots represent solvent molecules.

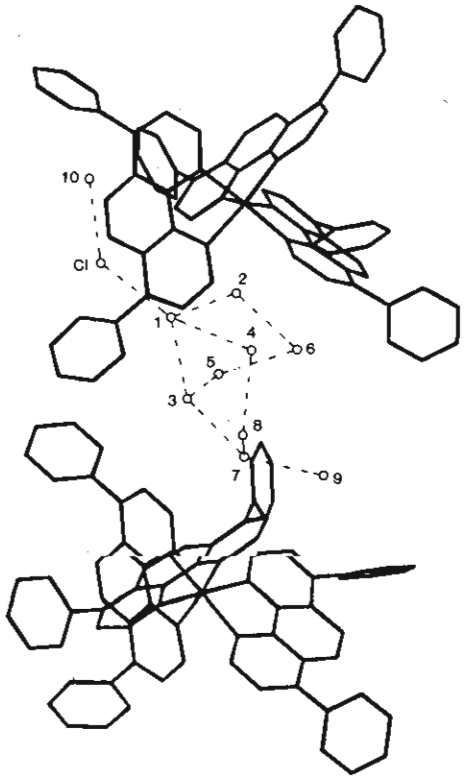

Figure 5. Solvent channel in the $Ru(DIP)_3^{2+}$ crystal. Dotted lines indicate solvent–solvent contacts less than 3.3 Å.

aligned along the major groove (Figure 6b).

Support for an intercalation model comes from the fact that it is known that $Ru(phen)_3^{2+}$, an analogue of $Ru(DIP)_3^{2+}$ that lacks the phenyl groups, binds to DNA by partial intercalation between the base pairs;[15] all spectroscopic data obtained to date show detailed similarities between the binding of $Ru(phen)_3^{2+}$ and that of $Ru(DIP)_3^{2+}$. In the proposed model, the phenyl group is positioned in the minor groove in a manner similar to that observed in the crystal structure of the complex between ethidium bromide and CpG.[16] In an earlier model[1a] for $Ru(DIP)_3^{2+}$–DNA binding, it was proposed that the entire diphenylphenanthroline moiety intercalates. This would require that the phenyl groups rotate into the plane of the phenanthroline moiety in order to maximize stacking. However, the crystal structure shows that all the phenyl groups are skewed; rotation of the plane of these groups within 40° of the phenanthroline plane produces unfavorable intramolecular contacts. The newly proposed model thus requires that the base pairs open up during the process of intercalation in order to accommodate the skewed phenyl group. This would suggest a slow association and dissociation of the complex from the helix, which time-resolved luminescence experiments may be able to confirm.

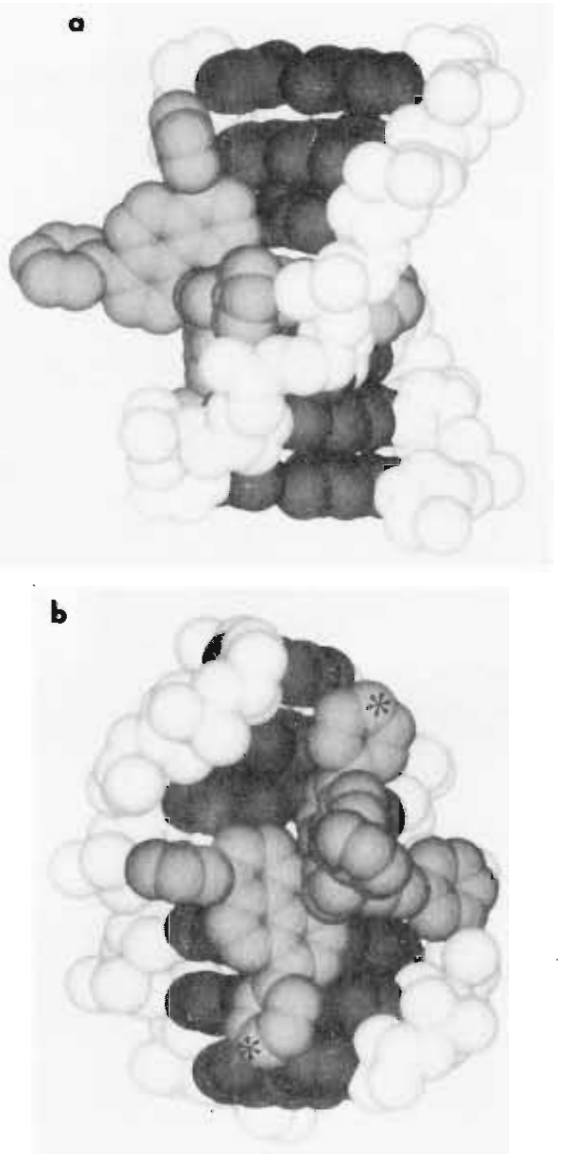

Figure 6. Model for the binding of $Ru(DIP)_3^{2+}$ to DNA: (a) view showing the intercalated ligands; (b) view down the approximate twofold helical axis (starred atoms define the vector along the major groove; see text). One phenanthroline ring is partially intercalated between two base pairs. The nonintercalating ligands lie along the major groove of DNA.

The nonintercalating ligands are involved in hydrophobic nonstacking interactions with the base pairs along the helical major groove. Evidence for major-groove binding for both $Ru(DIP)_3^{2+}$ and $Ru(phen)_3^{2+}$ comes from very recent experiments with glucosylated DNA.[17] The interactions in the model shown in Figure 6 are similar to those observed in the packing of the molecules of $Ru(DIP)_3^{2+}$ within the crystal. They are also seen in the complex between netropsin and dodecameric DNA,[18] although in that structure these interactions occur in the minor groove.

The proposed binding model accounts well for the stereospecificity seen in the binding to the right-handed B-DNA helix. Figure 6 shows the intercalated Δ-$Ru(DIP)_3^{2+}$ complex viewed perpendicular to the helix axis. A vector drawn between the two starred phenyl group atoms in Figure 6b is directed upward from

(8) Anderson, O. P. *J. Chem. Soc., Dalton Trans.* **1973**, 1237–1241.
(9) Zalkin, A.; Templeton, D. H.; Ueki, T. *Inorg. Chem.* **1973**, *12*(7), 1641–1646.
(10) Bonneson, P.; Walsh, J. L.; Pennington, W. T.; Cordes, A. T.; Durham, B. *Inorg. Chem.* **1983**, *22*, 1761–1765.
(11) Gould, R. O.; Stephenson, T. A.; Thomson, M. A. *J. Chem. Soc., Dalton Trans.* **1980**, 804–809.
(12) At one point in the refinement, the persistent appearance of solvent sites 7 and 8 were thought to be various combinations of disordered methanol and water molecules. It is not possible to either confirm or rule out this possibility.
(13) (a) Terzis, A. *Cryst. Struct. Commun.* **1978**, *7*, 95–99. (b) Sletten, E.; Ruud, M. *Acta Crystallogr., Sect. B: Struct. Crystallogr. Cryst. Chem.* **1975**, *B31*, 982–985. (c) Kistenmacher, T. J.; Shigematsu, T. *Acta Crystallogr., Sect. B: Struct. Crystallogr. Cryst. Chem.* **1974**, *B30*, 166–168. (d) Ito, M.; Marumo, F.; Saito, Y. *Acta Crystallogr., Sect. B: Struct. Crystallogr. Cryst. Chem.* **1971**, *B27*, 2187–2195. (e) Marumo, F.; Utsumi, Y.; Saito, Y. *Acta Crystallogr., Sect. B: Struct. Crystallogr. Cryst. Chem.* **1970**, *B26*, 1492–1498.
(14) Schlemper, E. O.; Fair, C. K. *Acta Crystallogr., Sect. B: Struct. Crystallogr. Cryst. Chem.* **1977**, *B33*, 2482–2489.
(15) Barton, J. K.; Danishefsky, A.; Goldberg, J. *J. Am. Chem. Soc.* **1984**, *106*, 2172–2176.
(16) Jain, S. C.; Tsai, C. C.; Sobell, H. M. *J. Mol. Biol.* **1977**, *114*, 317–331.
(17) Goldberg, J. M.; Kumar, C.; Barton, J. K., personal communication, 1985.
(18) Kopka, M. L.; Yoon, C.; Goodsell, D.; Pjeua, P.; Dickenson, R. E. *Proc. Natl. Acad. Sci. U.S.A.* **1985**, *82*, 1376–1380.

left to right along the helical groove. In the λ isomer this same vector is directed from right to left opposing the right-handed groove. This structural difference between the enantiomers leads to unfavorable contacts between the nonintercalating ligands on the λ isomer and the sugar phosphate backbone of the DNA double helix. Because the presence of the phenyl groups increases the number of these potential contacts, this model would account for the increase in chiral discrimination observed for $Ru(DIP)_3^{2+}$ in comparison to that for $Ru(phen)_3^{2+}$. Thus, this model may be useful both for designing new experiments and for developing new DNA binding agents of high site and conformation specificity.

Acknowledgment. This research was supported by the National Institutes of Health through Grants GM21589 (H.M.B.), CA06927 (H.M.B.), CA09035 (B.M.G.), RR05539 (H.M.B.), and GM33309 (J.K.B.) and through an appropriation from the Commonwealth of Pennsylvania. We thank Avis Danishefsky for preparation of the complex.

Registry No. $[Ru(DIP)_3]Cl_2$, 36309-88-3.

Supplementary Material Available: Listings of observed and calculated structure factors and thermal parameters for $Ru(DIP)_3^{2+}$ (18 pages). Ordering information is given on any current masthead page.

Contribution from the Department of Chemistry, Rutgers, The State University of New Jersey, New Brunswick, New Jersey 08903

Light-Induced Excited-Spin-State Trapping: Evidence from VTFTIR Measurements

R. Herber* and L. M. Casson

Received July 23, 1985

Samples of *cis*-$Fe(phen)_2(SCN)_2$ (phen = 1,10-phenanthroline) were examined by variable-temperature Fourier transform infrared spectroscopy over the range $8 \leq T \leq 310$ K. The room-temperature high-spin form and the low-spin form stable at liquid-nitrogen temperature can be readily distinguished by their characteristic infrared signatures, both in the ν_{CN} region ($\sim$2100 cm^{-1}) and in the spectral range 900–600 cm^{-1}. The high-spin–low-spin conversion in KBr as estimated from infrared intensities is approximately half-complete at 159 ± 5 K, a temperature ~20 K lower than that extracted from heat capacity, susceptibility, and ^{57}Fe Mössbauer data. When the sample is cooled to ~8 K, the low-spin form of the complex is converted to a high-spin form by optical pumping due to the 632.8-nm radiation of the He/Ne laser of the spectrometer. The high-spin form so produced by the LIESST process is stable in KBr, CsI, and TlBr matrices at low temperatures but is gradually transformed into a low-spin form on warming the samples above ~32 K. Both the thermodynamics and kinetics of the conversion processes between the several spin states of the ferrous complex can be conveniently followed by infrared spectroscopic techniques.

Introduction

The phenomenon of thermally driven spin crossover in first-row transition-metal complexes, with electron configurations d^4 to d^7, which was first demonstrated in tris(dithiocarbamato) complexes of Fe^{3+} by Cambi et al.,[1] has been extensively reviewed in the literature. In particular, the $^5T_2$ (high-spin, HS)–^1A (low-spin, LS) transition in *cis*-$Fe^{II}(phen)_2(SCN)_2$ has been studied in considerable detail by Gutlich et al.,[2-5] who have made use of ^{57}Fe Mössbauer spectroscopy and susceptibility measurements to characterize the temperature dependence of the transition from the $S = 2$ to the $S = 0$ configuration of the complex. The magnetic behavior of $Fe(phen)_2(SCN)_2$ had been originally observed by Baker and Bobonich,[6] who noted that the spin transition is very sharp and occurs at ~175 K in the solid, with little or no hysteresis during warming and cooling cycles. In particular it is interesting to note that not only is there the expected characteristic susceptibility difference between the HS and LS form of this compound but in addition both the Mössbauer and infrared signatures of the two spin states are significantly different and permit a detailed study of the thermodynamics of the crossover phenomenon. The relevant temperature-dependent data, especially as they pertain to the Mössbauer studies, have recently been reviewed by Gutlich.[5,7]

From such studies, it has become clear that if the subject samples are carefully prepared and treated prior to spectroscopic or susceptometric examination, complete conversion of the room-temperature HS form of $Fe(phen)_2(SCN)_2$ to the LS form can be achieved on cooling to liquid-nitrogen temperature. Of particular interest is the observation by Mössbauer techniques[8-10] that when the LS form is irradiated with white light at temperatures below ~50 K, a conversion to a form that has the Mössbauer spectral characteristics of the HS form can be achieved. This HS form, in turn, can be reconverted to the LS form by annealing the samples at temperatures of 30–32 K for short time periods. On recooling such annealed samples to liquid-helium temperatures in the dark, only the LS form spectroscopic parameters are observed. These transitions are schematically summarized in Figure 1, in which it is seen that the room-temperature form (HS-1) converts to the low-spin form (LS-1) on cooling to ~100 K. Further cooling, in the absence of optical excitations, to liquid-helium temperature, preserves the LS-1 form, which can then be converted to a high-spin form (HS-2) by optical pumping. When this metastable system is warmed above ~30 K, a reconversion to a low-spin form (LS-2), which is stable at ~100 K, is observed.

(1) Cambi, L.; Cagnasso, A. *Atti. Accad. Naz. Lincei, Cl. Sci. Fis., Mat. Nat., Rend.* **1931**, *13*, 809. Cambi, L.; Szego, L. *Ber. Dtsch. Chem. Ges. B* **1931**, *64*, 259.
(2) Gutlich, P. *Struct. Bonding (Berlin)* **1981**, *44*, 83. See also the review by: Konig, E.; Ritter, G.; Kulshreta, S. K. *Chem. Rev.* **1985**, *85*, 219 and references therein.
(3) Muller, E. W.; Spiering, H.; Gutlich, P. *Chem. Phys. Lett.* **1982**, *93*, 567.
(4) Ganguli, P.; Gutlich, P.; Muller, E. W.; Irler, W. *J. Chem. Soc. Dalton* **1981**, 441.
(5) Gutlich, P. In "Mössbauer Spectroscopy Applied to Inorganic Chemistry", Vol. 1, Long, G. J., Ed.; Plenum Press: New York, 1984; Vol. 1, Chapter XI, and references therein.
(6) Baker, W. A.; Bobonich, H. M. *Inorg. Chem.* **1964**, *3*, 1184.
(7) Gutlich, P. In "Chemical Mössbauer Spectroscopy"; Herber, R. H., Ed.; Plenum Press: New York, 1984; Chapter II.
(8) Decurtins, S.; Gutlich, P.; Kohler, C. P.; Spiering, H. *Chem. Phys. Lett.* **1984**, *105*, 1; *J. Chem. Soc. Chem. Commun.* **1985**, 430.
(9) Decurtins, S.; Gutlich, P.; Hauser, A.; Hasselbach, K. M.; Spiering, H. *Inorg. Chem.* **1985**, *24*, 2174.
(10) Decurtins, S.; Gutlich, P.; Kohler, C. P.; Spiering, H. *J. Chem. Soc., Chem. Commun.* **1985**, 430.

0020-1669/86/1325-0847$01.50/0